CHINESE OPTICS LETTERS

Vol. 19, No. 7 | July 2021

Three-nanosecond-equal interval sub-pulse Nd:YAG laser with multi-step active *Q*-switching

Jie Mao (毛 洁), Chao Wang (王 超)*, Tixiang Hong (洪梯翔), and Yongji Yu (于永吉)

Jilin Key Laboratory of Solid Laser Technology and Application, School of Science, Changchun University of Science and Technology, Changchun 130022, China

*Corresponding author: wangchaoopt@163.com

Received November 6, 2020 | Accepted December 19, 2020 | Posted Online April 12, 2021

We demonstrate a three-nanosecond equidistant sub-pulse multi-step *Q*-switched Nd:$Y_3Al_5O_{12}$ (Nd:YAG) laser. In the time interval of 100–1000 ns, three pulses with the same nanosecond interval and the same peak power are obtained at the pulse width of 24 ns, 28 ns, and 36.6 ns, respectively. The energy is 32.5 mJ, and the optical efficiency is 10.8%. The multi-step *Q*-switched method does not require the insertion of other optical elements into the traditional *Q*-switched laser, and it is very suitable to obtain pulse group output with several nanosecond pulse intervals.

Keywords: nanosecond interval pulse; multi-step *Q*-switching; Nd:YAG laser.

DOI: 10.3788/COL202119.071404

1. Introduction

The pulse laser, which can be widely used in different laser fields, has been reported in a large number of literatures[1–5]. The multi-pulse string laser can be obtained by selecting from high-frequency pulses. There are four methods to obtain the repetition pulse. Electro-optic *Q*-switched technology can produce multi-pulse lasers with high peak power, while the repetition frequency is relatively low [several hertz (Hz) to several thousand Hz][6]. Acousto-optic *Q*-switched technology can produce multiple pulse lasers with peak power of only kilowatts (kW), while the repetition frequency is several hundred kilohertz (kHz)[7,8]. Passive *Q*-switched technology can achieve an approximate output of acousto-optic *Q*-switched technology with poor stability[9]. Mode-locking technology can produce multiple pulse lasers with the repetition frequency of gigahertz (GHz)[10], while tiny pulse energy [about nanojoules (nJ)] and a complicated amplification system must be used. In conclusion, the electro-optic *Q*-switched, acousto-optic *Q*-switched, and passive *Q*-switched technologies have difficulty obtaining the frequencies above megahertz (MHz). Mode-locking technology has difficulty obtaining the frequency below GHz. Therefore, it is hardly impossible to achieve pulse group output with nanosecond pulse intervals.

In recent years, multi-pulsed lasers with nanosecond intervals have been used in laser-induced breakdown spectroscopy (LIBS), laser drilling, laser medical treatment, and other fields[11–16]. The several pulses of nanosecond intervals were achieved by a new method of controlling laser output delay[17–22]. In this method, a multi-channel signal generator is needed to control *Q*-switched delays for multiple lasers. The number of pulses depends on the number of multiple lasers, so the total size is large, and the price is expensive.

In this Letter, we demonstrate a three-nanosecond-equal interval sub-pulse Nd:$Y_3Al_5O_{12}$ (Nd:YAG) laser. Three-nanosecond-equal interval and peak-power-equal pulses were obtained in the time interval of 100–1000 ns. The pulse widths of the three sub-pulses fluctuate around 24 ns, 28 ns, and 36.6 ns, respectively, with an energy of 32.5 mJ and an optical efficiency of 10.8%. The multi-step *Q*-switched method does not require us to insert other optical elements into the traditional *Q*-switched laser; it is very suitable for obtaining pulse group outputs with several nanosecond pulse intervals.

We know that high-power pulses are usually obtained by *Q*-switched technology. The characteristics of the *Q*-switched method are first single energy storage and then actively normal lasing. The energy stored in the active medium before is suddenly released in the form of a very short pulse of light[23]. It is very difficult to accumulate the population inversion well above the threshold under nanosecond-interval pumping due to the microsecond time scale of fluorescence lifetime. This is also the reason for difficulty in obtaining nanosecond-interval pulse output by the traditional *Q*-switched technology.

In this paper, the method of obtaining multiple pulses by multi-step *Q*-switching is proposed, which has the characteristics of energy storage first and then multiple normal laser effects. Taking three-pulse output as an example, the process of multi-pulse output is illustrated. Figure 1 shows a typical time sequence for generating a three-step *Q*-switched pulse train. The resonant cavity loss presents a three-step distribution. The cavity

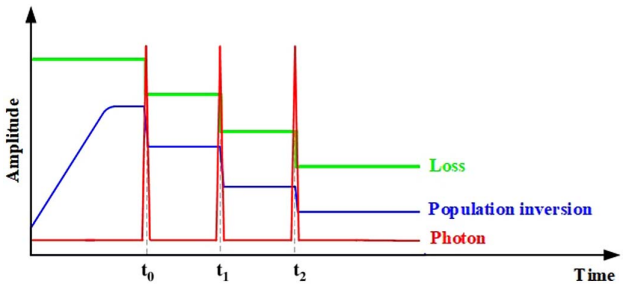

Fig. 1. Typical time sequence of the generation of three-step Q-switched pulses.

loss shows the first step decline at time t_0 after the population inversion reached peak values by the action of pumping. The population inversion is rapidly transformed into photons, and the first sub-pulse laser output is emitted. Then, after an appreciable delay $t_1 - t_0$, the resonator loss shows the second step decline, the population inversion is rapidly converted into the photons, and the second sub-pulse laser output is emitted. Finally, after an appreciable delay $t_2 - t_0$, the resonator loss drops in the third step, the population inversion drops again and turns into photons, and the third sub-pulse laser output is emitted. In order for the peak power of the three pulses to be equal, each step loss must be strictly controlled. For more pulses output, more step distribution is needed for the cavity loss, and each step loss must be strictly controlled. Multiple nanosecond pulse intervals can be obtained without consequently reaccumulating the population inversion.

2. Materials and Methods

A three-pulse output is designed to verify the method. The experimental setup of the three-nanosecond-interval sub-pulse laser is illustrated in Fig. 2. The laser system includes a diode-pumped module, a laser resonator, an electro-optic switch, a Q-switched driver, and an LD power supply. In order to obtain a three-pulse laser output, it is necessary for the diode-pumped module to maintain a sufficiently high gain. The structure of an annular side-pumped Nd:YAG rod[24–26] is adopted consequently, which allowed more bars to be arranged along the annular surface. The Nd:YAG rod with doping concentration of 1.0% (atomic fraction) is used as the laser gain medium, both end faces are coated with 1064 nm anti-reflective (AR) coating, and its size is $\phi 4 \times 25\ \mathrm{mm}^3$. The total peak power of the ten bars, which have an 808 nm center wavelength and 3.2 nm linewidth, is up to 1500 W. The two end segments wrapped with 0.05 mm indium foil are attached to the copper heat sink blocks. The laser resonator is a typical convex-plane cavity configuration, whose length is fixed at 300 mm. The mirror (M1) with high reflectivity ($>$ 99.8%) at 1064 nm is a plano-convex mirror with curvature radius of 2000 mm. The output coupler (M2) with reflectivity of 50% at 1064 nm is a plane mirror. The electro-optic switcher includes a polarizer and an electro-optic crystal. The polarizer is inserted to make the inter-cavity light with polarization

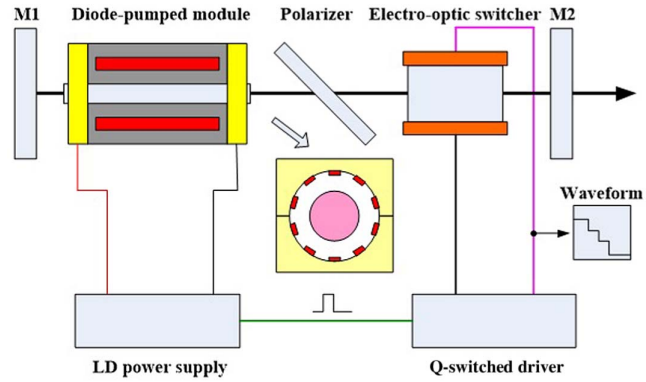

Fig. 2. Diagram of three-nanosecond-interval sub-pulse laser.

properties. The electro-optic crystal uses a lithium niobate (LN) with crystal size of 6 mm × 6 mm × 20 mm and quarter-wave voltage about 2000 V. The Q-switched driver is a three-fall-voltage step driver. The three-fall-voltage time intervals can be adjusted between 50 ns and 1200 ns. The adjustment voltage range is between 0 V and 3 kV. The number and amplitude of the fall-voltage can be regulated by the user. The laser diode (LD) power supply has the capability of 200 μs pulse width, 20 Hz repetition frequency, and 100 A current output, ensuring that the maximum pumping energy reaches 300 mJ. An additional square wave signal to trigger the Q-switched driver is output at the end of the current output.

The voltage goes down three steps (Fig. 2). Each of these steps has the same time interval (Δt). At the three-step voltage drop, the loss in the laser cavity can be written as

$$\gamma(t) = \delta_1 + \ln\left(\frac{1}{R}\right) + \ln\left\{\frac{1}{\cos^2\left[\frac{\pi V(t)}{2V_{\lambda/4}}\right]}\right\} \times \begin{cases} V_1, & t_0 < t \le t_1 \\ V_2, & t_1 < t \le t_2 \\ 0, & t_2 < t \end{cases}, \tag{1}$$

where δ_1 is the resonator loss factor, R is the reflectivity of the output mirror, $V_{\lambda/4}$ is the quarter-wave voltage, and $V(t)$ is the voltage on the electro-optic crystal, which has a great influence on the pulse output. Because of the three orders of magnitude between the nanosecond interval and the fluorescence lifetime of Nd:YAG, the nanosecond loss can be ignored. The first pulse is determined by the initial laser gain and the corresponding loss V_1, the second pulse is determined by the final laser gain of the first pulse and the corresponding loss V_2, and the third pulse is mainly determined by the termination laser gain of the second pulse and the corresponding loss zero voltage. On the premise of ensuring three-pulse output, these voltages can be further optimized to obtain peak-power-equal pulses. The performance of the laser is studied by measuring the energy and pulse width. The high-voltage probe (Tektronix P6015A) is used to measure the high-voltage signal of the Q-switched driver. The energy meter (Nova II + PE50) is used to measure the output energy. The photo detector (Thorlabs DET10A1M) and the oscilloscope (DPO3054) are used to measure the laser output waveform. The

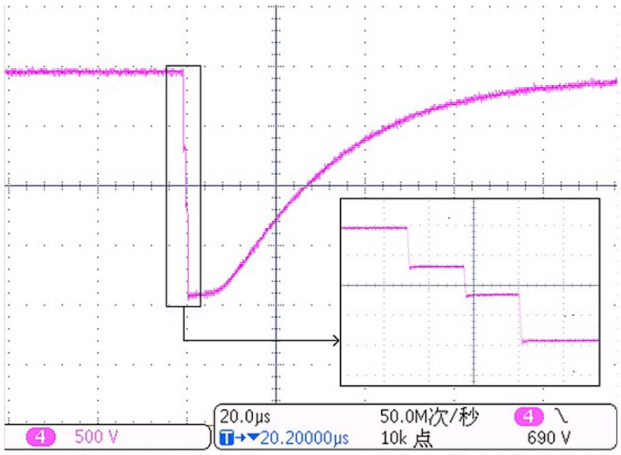

Fig. 3. Waveform of electro-optic Q-switching.

sub-pulse time intervals are controlled by the Q-switched driver. The voltage of each step was adjusted to obtain the same peak power of the three sub-pulses. Figure 3 shows the voltage waveform of the electro-optic switching. The time for the voltage from 2000 V to 0 V is about 100 μs. The fall voltage waveform is enlarged in a black frame. The descent edge of each step is about 10 ns, and the step duration is 400 ns.

3. Experimental Results and Analysis

Firstly, the performance of traditional Q-switching is studied before the method is used. Figure 4 shows the performance of the traditional Q-switching. The pump threshold is about 5.78 mJ, and the slope is about 22%. The output energy of 63 mJ is achieved at the maximum input of 300 mJ. The corresponding optical efficiency is 21%. The waveform is displayed at the maximum input, and the pulse width of 22.85 ns is obtained. The initial gain under different inputs is also shown in Fig. 4. The initial gain is estimated from the model of laser output. At the maximum input, the initial gain is up to 2.5 cm^{-1}.

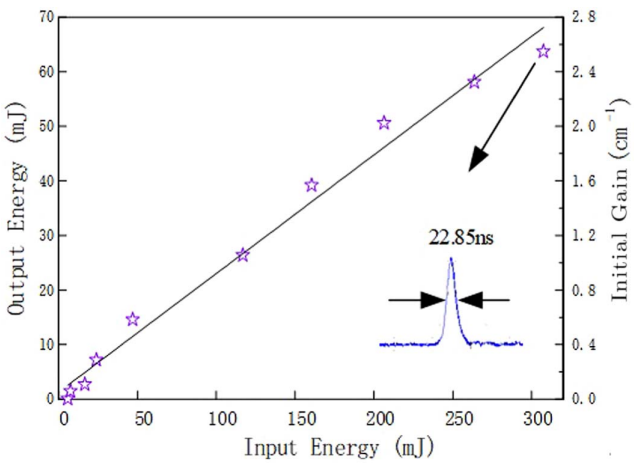

Fig. 4. Performance of conventional Q-switching.

Secondly, the performance of three-step Q-switching is studied. Observing the pulse group waveform, the two voltages of 1280 V (V_1) and 800 V (V_2) are selected at the maximum input, ensuring the same peak power of three pulses. The waveforms of the pulse group at the time interval between 50 ns and 1050 ns are measured. The descent edge of each step is about 10 ns. The three pulses at 50 ns time intervals cannot be distinguished, so the minimum time interval is 100 ns. When the time interval goes up above 1000 ns (1050 ns), some small pulses occasionally appear between the three sub-pulse intervals. The group waveforms at several typical time intervals of 100 ns, 200 ns, 300 ns, 500 ns, 700 ns, and 1050 ns are given in the Fig. 5. Except for the 1050 ns time interval, the pulses of each time interval have almost the same amplitude, which indicates the same peak power. When the pulse interval is greater than 1000 ns, some small pulses occasionally appear. Therefore, the time interval between the three stable pulses is 100–1000 ns.

The pulse widths of the three pulses are measured at different time intervals, as shown in Fig. 6. The pulse width and group energy have little change with the different time intervals. The pulse width fluctuates around 24 ns, 28 ns, and 36.6 ns,

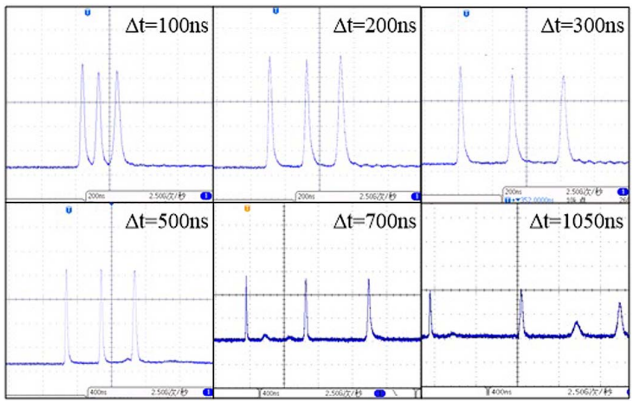

Fig. 5. Three sub-pulse output sequence with different time intervals.

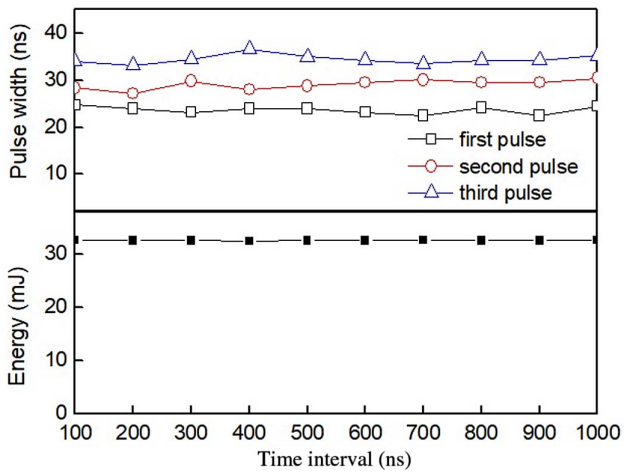

Fig. 6. Pulse width and energy of the three pulses versus pulse interval.

respectively. The pulse group energy is about 32.5 mJ, and the optical efficiency is 10.8%. This is because the fluorescence lifetime of the gain media (YAG) is about 200 μs, and the population inversion defect of nanoseconds can be ignored. This is consistent with the previous hypothesis. Compared with the traditional Q-switching, the pulse energy and the extraction efficiency are reduced, which is due to the first two sub-pulses being output at high cavity losses. It is almost impossible to directly measure the energy of each pulse in the nanosecond-interval pulse group. Based on the same peak power and the ratio of the three pulse widths, the energy of the three sub-pulses is estimated to be 8.77 mJ, 10.40 mJ, and 13.32 mJ, respectively. The peak power of the three sub-pulses is estimated to reach 360 kW. With the change of pump frequency (1 Hz to 20 Hz), the output pulse interval and peak power of sub-pulses have little change.

In order to obtain approximate pulsed laser output, we can regard multi-step Q-switching as a composition of many ideal Q-switching processes; the Q-switched equation is shown below:

$$\frac{\mathrm{d}\phi}{\mathrm{d}t} = \frac{2\sigma n l \phi}{t_r} - \frac{\phi}{t_c(t)}, \tag{2}$$

$$\frac{\mathrm{d}n}{\mathrm{d}t} = -\gamma\sigma c \phi n, \tag{3}$$

where t_c is the lifetime of photons in the cavity, t_r is the cavity round-trip time, and its function form is

$$t_c(t) = \frac{t_r}{L(t)}, \qquad \text{with} \quad L(t) = \begin{cases} L_1, & t_0 < t \le t_1 \\ L_2, & t_1 < t \le t_2 \\ L_3, & t_2 < t \le \infty \end{cases}. \tag{4}$$

According to the above relationship, the sizes of L_1, L_2, and L_3 are optimized to achieve the approximate sub-pulse laser output. By analyzing the expression of peak power in Q modulation and using the relationship of $g = n\sigma$ in the four-level system, new expressions of peak power are obtained:

$$P_{\mathrm{peak},m} = \frac{h\nu A l}{\sigma t_r} \ln\left(\frac{1}{R}\right)\left(g_{i,m} - g_{\mathrm{th},m} - g_{\mathrm{th},m} \ln\frac{g_{i,m}}{g_{\mathrm{th},m}}\right), \tag{5}$$

where m stands for any pulse, σ is the stimulated emission cross section, $h\nu$ is the laser photon energy, and A is the effective beam cross-sectional area. R is the output mirror reflectivity. According to the numerical relationship of the initial gain g_i, the threshold gain g_{th} and g' in Eq. (6),

$$g_i - g_{\mathrm{th}} = g' \ln\left(\frac{g_i}{g_{\mathrm{th}}}\right), \tag{6}$$

the expression of peak power can be expressed as

$$P_{\mathrm{peak}} = \frac{h\nu A l}{\sigma t_r} \ln\left(\frac{1}{R}\right)(g' - g_{\mathrm{th}}) \ln\left(\frac{g_i}{g_{\mathrm{th}}}\right). \tag{7}$$

The peak powers of the three pulses are equal, so the condition of equal peak power is the product of

$$(g' - g_{\mathrm{th}}) \ln\left(\frac{g_i}{g_{\mathrm{th}}}\right) = C, \tag{8}$$

where C is a fixed value, and g' can be obtained by combining Eqs. (6) and (8). If the initial gain g_i of the first pulse is given, the gain threshold g_{th} can be obtained. Then, combined with Eq. (9),

$$g_i - g_f = g_{\mathrm{th}} \ln\left(\frac{g_i}{g_f}\right), \tag{9}$$

the final gain g_f of the first pulse can be obtained, which is also used as the initial gain g_i of the second pulse. The relationship between the initial gain g_i and the final gain g_f of each pulse is calculated.

Thus, the pulse width and pulse energy of each pulse can be calculated:

$$t_p = t_r \frac{g_i - g_f}{g_i - g_{\mathrm{th}}[1 + \ln(g_i/g_{\mathrm{th}})]}, \tag{10}$$

$$E_{\mathrm{out}} = \frac{h\nu A}{2\sigma\gamma} \ln\left(\frac{1}{R}\right) \ln\left(\frac{g_i}{g_f}\right). \tag{11}$$

According to the equalization condition of peak power (360 kW), the relationship between threshold gain, initial gain, and termination gain is obtained by numerical simulation (Fig. 7). The three values of the threshold gain are 1.92 cm^{-1}, 1.23 cm^{-1}, and 0.75 cm^{-1}, which are basically consistent with the losses (1.992, 1.16, and 0.74) calculated by Eq. (1) at the voltages of 1280 V, 800 V, and 0 V. The energy of the three pulses is determined by the $\ln(n_i/n_f)$ of each stage through analyzing the expression of output energy[27]. The pulse energy and pulse width show a trend of gradual increasing, which agrees with the experimental results. Using the analytical method, we further discussed the feasibility of obtaining more pulses. With the initial gain of 2.5 cm^{-1}, eight, six, four, and three pulses would be obtained at the four peak powers of 40 kW, 80 kW, 180 kW, and 360 kW, respectively. Therefore, the number of pulses can be increased by reducing the peak power. If the initial

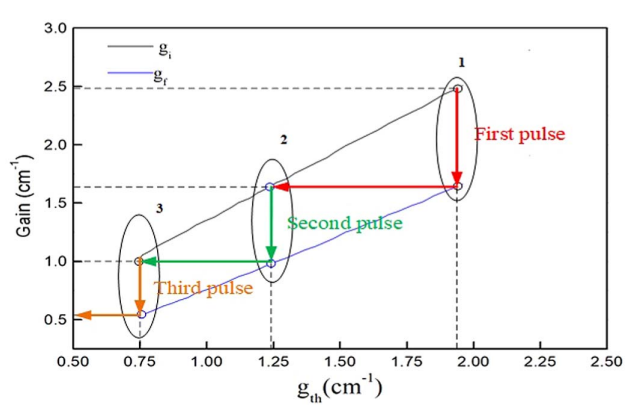

Fig. 7. Relationship of g_{th} and g_i, g_f at the peak power of 360 kW.

gain is further increased, the number of pulses will be further increased.

4. Conclusions

In summary, we presented the method of achieving multiple nanosecond-interval pulses based on multi-step *Q*-switching, which has the characteristics of single energy storage first and then multiple normal lasing actions. The method was applied to the traditional *Q*-switched Nd:YAG laser. The three-pulse group with 360 kW peak power was obtained stably at time intervals between 100 ns and 1000 ns, which is hardly impossible to achieve by adopting traditional *Q*-switching methods. The total energy of the group is about 32.5 mJ, and the corresponding optical efficiency is 10.8%. The pulse widths of three pulses are 24 ns, 28 ns, and 36.6 ns, respectively. The three-pulse energies show a trend of gradual increasing, which agrees with the numerical simulation. The number of pulses can be increased by increasing the initial gain and decreasing the peak power by numerical analysis. The method shows that the multi-step *Q*-switching method, which we presented, is practicable for achieving nanosecond-interval sub-pulses. Compared with other methods of achieving nanosecond-interval pulses, it is simple without inserting other optical elements in conventional *Q*-switched lasers, which provides a new way for pulse group outputs with several nanosecond pulse intervals.

Acknowledgement

This work was supported by the National Natural Science Foundation of China (NSFC) (No. 11974060) and the Natural Science Foundation of Jilin Province (No. 20190201266JC).

References

1. B. R. Anderson, R. Gunawidjaja, N. Gese, and H. Eilers, "Two-color thermometric imaging of heterogeneous materials during pulsed laser heating," Appl. Phys. B **126**, 158 (2020).
2. J. Kou, Y. Wang, X. Liu, X. Zhang, G. Chen, X. Xu, J. Bao, K. Yang, and L. Yuwen, "Continuous preparation of antimony nanocrystals with near infrared photothermal property by pulsed laser ablation in liquids," Sci. Rep. **10**, 15095 (2020).
3. H. C. Zhao, Y. L. Qiao, X. Du, S. J. Wang, Q. Zhang, and Y. Zang, "Research on the technology of paint removal for aluminum alloy by pulsed laser," Chin. J. Lasers **48**, 0302001 (2021).
4. M. Wang, F. Wang, S. Feng, C. Yu, S. Wang, Q. Zhou, L. Zhang, F. Lou, D. Chen, and L. Hu, "272 W quasi-single-mode picosecond pulse laser of ytterbium-doped large-mode-area photonic crystal fiber," Chin. Opt. Lett. **17**, 071401 (2019).
5. C. Wang, Q. Peng, L. Xin, and J. Liu, "Active–passive pulse laser based on gold nanobipyramids at 1.3 μm wavelength," Chin. Opt. Lett. **17**, 020003 (2019).
6. B. B. Boiko, N. S. Petrov, V. V. Valyavko, and I. M. Vashkevich, "Polarizers for lasers with electrooptic *Q*-switches," J. Appl. Spectrosc. **8**, 319 (1968).
7. C. Wang, T. X. Hong, S. T. Li, Y. J. Yu, and G. Y. Jin, "A highly-efficient double pass Nd:YVO_4 master oscillator power amplifier," Laser Phys. **29**, 095002 (2019).
8. R. I. Woodward, M. R. Majewski, N. Macadam, G. Hu, T. Albrow-Owen, T. Hasan, and S. D. Jackson, "*Q*-switched Dy:ZBLAN fiber lasers beyond 3 μm: comparison of pulse generation using acousto-optic modulation and inkjet-printed black phosphorus," Opt. Express **27**, 15032 (2019).
9. S. A. Mikhnov, V. A. Kononov, R. V. Mikhnova, and L. S. Korochkin, "Temporal development of pulses in lasers with passive *Q*-switches," J. Appl. Spectrosc. **33**, 694 (1980).
10. E. Hernandez-Escobar, M. Bello-Jimenez, R. Lopez-Estopier, A. Camarillo-Aviles, O. Pottiez, M. A. Garcia-Ramirez, M. Duran-Sanchez, B. Ibarra-Escamilla, and M. V. Andres, "*Q*-switching and mode locking pulse generation from an all-fiber ring laser by intermodal acousto-optic bandpass modulation," Laser Phys. **29**, 015101 (2019).
11. S. Li, Q. Wang, R. Song, F. Hou, and C. Gao, "Laser diode pumped high-energy single-frequency Er:YAG laser with hundreds of nanoseconds pulse duration," Chin. Opt. Lett. **18**, 031401 (2020).
12. X. J. Wang, F. Y. Meng, M. Li, J. B. Wang, and G. B. Gao, "Nanosecond dual pulse laser controlling method," Chin. J. Lasers **38**, 0203004 (2011).
13. X.-D. Wang, A. Michalowski, F. Dausinger, and J.-S. Liu, "Double-pulse technique for short pulse laser drilling," Laser Tech. **33**, 283 (2009).
14. X. K. Miao, W. Zhao, H. W. Zhang, and W. H. Yang, "Research of laser encoding method based on time-controlled pulse interval," Infrared Laser Eng. **45**, 1006002 (2016).
15. X. D. Wang, A. Michalowski, D. Walter, S. Sommer, M. Kraus, J. S. Liu, and F. Dausinger, "Laser drilling of stainless steel with nanosecond double-pulse," Opt. Laser Technol. **41**, 148 (2009).
16. C.-Z. Liu, Y.-P. Dou, L. Zhang, C.-K. Sun, Z.-Q. Hao, and J.-Q. Lin, "Research on the dynamics of ion debris from Sn plasma by use of dual laser pulses," Spectrosc. Spect. Anal. **35**, 44 (2015).
17. D. Salehinia, M. Farahmandjou, K. Khorasani, and S. Behrouzinia, "The continuous control of output power of a CuBr laser by a pulsed external magnetic field," Opt. Commun. **436**, 143 (2019).
18. L. Shu, Y. Li, L. Chen, J. Shi, L. Chai, C. Wang, A. B. Fedotov, and A. M. Zheltikov, "Quarter-cycle engineering of terahertz field waveforms," Laser Phys. Lett. **11**, 085404 (2014).
19. P. B. Meng, B. Q. Yao, G. Li, Y. L. Ju, and Y. Z. Wang, "Comparison of RTP electro-optic *Q*-switch and acousto-optic *Q*-switch in Tm, Ho:$GdVO_4$ laser," Laser Phys. **21**, 348 (2011).
20. M. Delgado-Pinar, D. Zalvidea, A. Diez, P. Perez-Millan, and M. Andres, "*Q*-switching of an all-fiber laser by acousto-optic modulation of a fiber Bragg grating," Opt. Express **14**, 1106 (2006).
21. J. R. Negri, F. Pirzio, and A. Agnesi, "Passively *Q*-switched single-frequency Nd:YVO_4 ring laser with external feedback," Opt. Express **26**, 11903 (2018).
22. C. Gordon, M. Cumbajin, G. Carpintero, E. Bente, and J. Javaloyes, "Absorber length optimization of on-chip colliding pulse mode-locked semiconductor laser," IEEE J. Sel. Top. Quantum Electron. **24**, 1100808 (2018).
23. Q. Y. Zeng, Y. Wan, J. C. Xiong, and D. Y. Zhu, "Modeling the pulse shape of *Q*-switched lasers to account for terminal-level relaxation," Chin. Phys. B **20**, 034204 (2011).
24. S. Fujikawa, K. Furuta, and K. Yasui, "28% electrical-efficiency operation of a diode-side-pumped Nd:YAG rod laser," Opt. Lett. **26**, 602 (2001).
25. W. Wang, C. Fu, Z. Hu, Q. Zhao, and M. Gong, "Segment side-pumped *Q*-switched Nd:YAG laser," Appl. Opt. **51**, 1765 (2012).
26. Z. X. Bai, X. Q. Gao, L. Y. Chen, J. Jiang, M. Chen, and G. Li, "Development of a high power *Q*-switched laser diode-pumped Nd:YAG master oscillator power amplifier (MOPA) laser with high repetition rate," Laser Eng. **28**, 233 (2014).
27. J. J. Degnan, "Theory of the optimally coupled *Q*-switched laser," IEEE J. Quantum Electron. **25**, 214 (1989).